

Nuclear electromagnetic processes in ChEFT

L Girlanda^{1,2}, L E Marcucci^{3,4}, S Pastore⁵, M Piarulli⁶,
R Schiavilla^{6,7}, M Viviani⁴

¹ Department of Mathematics and Physics, University of Salento, I-73100 Lecce, Italy

² INFN, Sezione di Lecce, I-73100 Lecce, Italy

³ Department of Physics, University of Pisa, I-56127 Pisa, Italy

⁴ INFN, Sezione di Pisa, I-56127 Pisa, Italy

⁵ Department of Physics and Astronomy, University of South Carolina, Columbia, SC 29208, USA

⁶ Department of Physics, Old Dominion University, Norfolk, VA 23529, USA

⁷ Theory Center, Jefferson Laboratory, Newport News, VA 23606, USA

E-mail: girlanda@le.infn.it

Abstract. We review our recent work on the derivation of the nuclear electromagnetic charge and current operators in chiral perturbation theory, based on time-ordered perturbation theory. We then discuss the strategies for fixing the relevant low-energy constants, and compare the resulting predictions for the electric and magnetic form factors of the deuteron and trineutrons with experimental data, using as input accurate nuclear wave functions derived with realistic potentials.

1. Introduction

Besides providing a justification for the hierarchy of nuclear forces, establishing a clear contact with the underlying theory of strong interaction and its symmetries, and leading to a well defined expansion scheme, susceptible of systematic improvement, the chiral effective field theory (χ EFT) is ideally suited for deriving consistent electroweak currents. Indeed, chiral perturbation theory is formulated as an effective theory of external currents, which are coupled to the degrees of freedom of the fundamental theory. The constraints imposed by chiral symmetry, so-called chiral Ward identities, are obtained promoting the global chiral symmetry to a local one [1], with the external currents r_μ and ℓ_μ , representing the corresponding gauge fields. The explicit breaking of chiral symmetry by quark masses and electromagnetic currents is naturally implemented: correlation functions are to be evaluated with the scalar source χ proportional to the quark mass matrix and the external currents set equal to the photon field, $r_\mu = \ell_\mu = QA_\mu$ with $Q = e \text{diag}(\frac{2}{3}, -\frac{1}{3})$ in the meson sector and $Q = e \text{diag}(1, 0)$ in the nucleon sector. Indeed, soon after the Weinberg proposal [2] in the 90s, electroweak transition operators have been addressed by Park, Min and Rho [3], using covariant perturbation theory. Nuclear electromagnetic currents and charge operators have recently been rederived in time-ordered perturbation theory [4, 5, 6, 7] and in the so-called unitary transformation method [8, 9] within the same scheme as for the NN potential [10] based on the Okubo procedure [11]. The similarities and differences among these approaches are discussed in Refs. [4, 5, 9]. In what follows we describe the approach based on time-ordered perturbation theory (TOPT).



The effective Lagrangian is the most general one invariant under chiral symmetry: it contains an infinite number of operators, classified according to the chiral counting, a combined expansion in powers of quark masses and small momenta, with $\chi \sim O(p^2)$. The chiral counting is thus the organizing principle: it works because Goldstone bosons have derivative interactions, as dictated by the Goldstone's theorem. From the chiral Lagrangian (see Ref. [12]), the canonical formalism allows to obtain the Hamiltonian which describes the interactions of pions, nucleons and photons. For the present discussion the following contributions are relevant

$$H_{\pi N} = \int d\mathbf{x} N^\dagger \left[\frac{g_A \tau_a}{F_\pi} \boldsymbol{\sigma} \cdot \nabla \pi_a + \frac{\boldsymbol{\tau}}{F_\pi^2} \cdot (\boldsymbol{\pi} \times \partial^0 \boldsymbol{\pi}) + \dots \right] N, \quad (1)$$

$$H_{\gamma N} = e \int d\mathbf{x} N^\dagger \left[e_N A^0 + i \frac{e_N}{2m} \left(-\overleftarrow{\nabla} \cdot \mathbf{A} + \mathbf{A} \cdot \overrightarrow{\nabla} \right) - \frac{\mu_N}{2m} \boldsymbol{\sigma} \cdot \nabla \times \mathbf{A} - \frac{2\mu_N - e_N}{8m^2} \left(\nabla^2 A^0 + \boldsymbol{\sigma} \times \nabla A^0 \cdot \overrightarrow{\nabla} - \overleftarrow{\nabla} \cdot \boldsymbol{\sigma} \times \nabla A^0 \right) + \dots \right] N, \quad (2)$$

$$H_{\gamma\pi} = e \int d\mathbf{x} \left[A^0 (\boldsymbol{\pi} \times \partial^0 \boldsymbol{\pi})_z + \epsilon_{zab} \pi_a (\nabla \pi_b) \cdot \mathbf{A} + \dots \right], \quad (3)$$

$$H_{\gamma\pi N} = e \int d\mathbf{x} N^\dagger \left[-\frac{g_A}{F_\pi} (\boldsymbol{\tau} \times \boldsymbol{\pi})_z \boldsymbol{\sigma} \cdot \mathbf{A} + \frac{g_A}{2m F_\pi} (\boldsymbol{\tau} \cdot \boldsymbol{\pi} + \pi_z) \boldsymbol{\sigma} \cdot \nabla A^0 + \left(\frac{d'_8}{F_\pi} \nabla \pi_z + \frac{d'_9}{F_\pi} \tau_a \nabla \pi_a + \frac{d'_{21}}{F_\pi} \epsilon_{zab} \tau_b \boldsymbol{\sigma} \times \nabla \pi_a \right) \cdot \nabla \times \mathbf{A} + \dots \right] N. \quad (4)$$

Here g_A is the nucleon axial coupling, F_π the pion decay constant, e the proton electric charge and m the nucleon mass, while the parameters d_i are (unknown) low-energy constants (LECs). $\boldsymbol{\sigma}$ and $\boldsymbol{\tau}$ are the spin and isospin Pauli matrices, and the isospin operators e_N and μ_N are defined as

$$e_N = (1 + \tau_z)/2, \quad \kappa_N = (\kappa_S + \kappa_V \tau_z)/2, \quad \mu_N = e_N + \kappa_N, \quad (5)$$

with κ_S and κ_V denoting the isoscalar and isovector combinations of the anomalous magnetic moments of the proton and neutron. The non-relativistic nucleon field N is an isospin doublet, while pions are described by the isovector $\boldsymbol{\pi}$ and photons by the four-vector A^μ . The chiral dimension of the resulting vertices is obtained by counting the powers of Q , the low-momentum scale, or equivalently the number of gradients, e.g. the two terms in $H_{\pi N}$ are each of order $\sim Q$, while the first terms in $H_{\gamma\pi N}$ are of order $\sim e Q^0$ and $\sim e Q$, and the remaining ones in second line of equation (4) are of order $\sim e Q^2$.

The two-nucleon contact Hamiltonian can be written as

$$H_{CT} = \int d\mathbf{x} \left[\frac{1}{2} C_S N^\dagger N N^\dagger N + \frac{1}{2} C_T N^\dagger \boldsymbol{\sigma} N \cdot N^\dagger \boldsymbol{\sigma} N - \frac{1}{32} (16C_1 - C_2 - 3C_4 - C_7) \nabla^2 (N^\dagger N) N^\dagger N + \frac{1}{32} (C_2 + 3C_4 + C_7) \nabla^2 (N^\dagger \tau^a N) N^\dagger \tau^a N - \frac{1}{32} (16C_3 - C_2 + C_4 + C_7) \nabla^2 (N^\dagger \sigma^i N) N^\dagger \sigma^i N + \frac{1}{32} (C_2 - C_4 - C_7) \nabla^2 (N^\dagger \sigma^i \tau^a N) N^\dagger \sigma^i \tau^a N - \frac{i}{8} C_5 \left[\overrightarrow{\nabla} \cdot (N^\dagger \overleftarrow{\nabla} \times \boldsymbol{\sigma} N) N^\dagger N - N^\dagger \overleftarrow{\nabla} N \cdot \overrightarrow{\nabla} \times (N^\dagger \boldsymbol{\sigma} N) \right] + \frac{1}{16} (8C_6 - C_7) \overrightarrow{\nabla} \cdot (N^\dagger \boldsymbol{\sigma} N) \overrightarrow{\nabla} \cdot (N^\dagger \boldsymbol{\sigma} N) - \frac{1}{16} C_7 \overrightarrow{\nabla} \cdot (N^\dagger \boldsymbol{\sigma} \tau^a N) \overrightarrow{\nabla} \cdot (N^\dagger \boldsymbol{\sigma} \tau^a N) \right], \quad (6)$$

where, inside a fermion bilinear, $\overleftrightarrow{\nabla} = \overrightarrow{\nabla} - \overleftarrow{\nabla}$. Here relativistic corrections [13] have been ignored, while the definition of the LECs C_i , typically determined by fitting low-energy two-nucleon scattering data and the deuteron binding energy, is chosen so as to conform to standard notation. In addition, Fierz identities have been used such that the resulting nucleon-nucleon potential can be put in local form [14]. Minimal substitution in this Hamiltonian, $\nabla N \rightarrow (\nabla - i e e_N \mathbf{A}) N$ in H_{CT} leads to a (contact) Hamiltonian $H_{CT}^{\gamma m}$ which includes the coupling to the EM field and implies a (two-nucleon) contact current operator. It is also necessary to consider non-minimal couplings, entering through the electromagnetic field tensor $F_{\mu\nu}$. The only two independent operator structures are

$$H_{CT}^{\gamma m} = e \int d\mathbf{x} \left[C'_{15} N^\dagger \boldsymbol{\sigma} N N^\dagger N + C'_{16} \left(N^\dagger \boldsymbol{\sigma} \tau_z N N^\dagger N - N^\dagger \boldsymbol{\sigma} N N^\dagger \tau_z N \right) \right] \cdot \nabla \times \mathbf{A} ,$$

where the isoscalar C'_{15} and isovector C'_{16} LECs (as well as the d_i 's multiplying the higher order terms in the $\gamma\pi N$ Hamiltonian) can be determined by fitting photo-nuclear data in few-nucleon systems.

2. From amplitudes to potentials

A generic transition amplitude, e.g. the two-nucleon scattering amplitude, can be calculated from the above Hamiltonians in the conventional TOPT, as

$$\langle f | T | i \rangle = \langle f | H_1 \sum_{n=1}^{\infty} \left(\frac{1}{E_i - H_0 + i\eta} H_1 \right)^{n-1} | i \rangle , \quad (7)$$

with $|i\rangle$ and $|f\rangle$ representing the initial and final NN states of energy $E_i = E_f$, H_0 the free Hamiltonian of pions and nucleons and H_1 containing the interactions. The time-ordered diagrams are obtained inserting complete sets of H_0 eigenstates between successive terms of H_1 . The infinite number of contributions are ordered according to the power counting in powers of $Q/\Lambda_\chi \ll 1$, where Q is the generic pion momentum and $\Lambda_\chi \simeq 1$ GeV is the typical hadronic mass scale, i.e. the mass of the states not protected by chiral symmetry.

A generic contribution in the perturbative series, equation (7), is characterized by a certain number N of vertices, each scaling as $Q^{\alpha_i} \times Q^{-\beta_i/2}$ ($i=1, \dots, N$), where α_i is the power counting implied by the relevant interaction Hamiltonian and β_i is the number of pions attached to the vertex, a corresponding $N-1$ number of energy denominators, and possibly L loops. Out of these $N-1$ energy denominators, N_K will involve only nucleon kinetic energies, which scale as Q^2 , and the remaining $N - N_K - 1$ will involve, in addition, pion energies, which are of order Q . Loops contribute a factor Q^3 each, since they imply integrations over intermediate three momenta. Hence the power counting associated with such a contribution is

$$\left(\prod_{i=1}^N Q^{\alpha_i - \beta_i/2} \right) \times \left[Q^{-(N - N_K - 1)} Q^{-2N_K} \right] \times Q^{3L} . \quad (8)$$

Each of the $N - N_K - 1$ "large" energy denominators can in turn be expanded as

$$\frac{1}{E_i - E_I - \omega_\pi} = -\frac{1}{\omega_\pi} \left[1 + \frac{E_i - E_I}{\omega_\pi} + \frac{(E_i - E_I)^2}{\omega_\pi^2} + \dots \right] , \quad (9)$$

where E_I denotes the kinetic energy of the intermediate two-nucleon state, ω_π the pion energies, and the ratio $(E_i - E_I)/\omega_\pi$ is of order Q . As a result the two-nucleon scattering amplitude T can be expanded as

$$T = T^{(0)} + T^{(1)} + T^{(2)} + \dots , \quad (10)$$

where $T^{(n)} \sim Q^n$. We can define a two-nucleon potential v such that, when iterated in the Lippmann-Schwinger (LS) equation,

$$v + v G_0 v + v G_0 v G_0 v + \dots , \quad (11)$$

with G_0 the free two-nucleon propagator, $G_0 = 1/(E_i - E_f + i\eta)$, it leads to the on-the-energy-shell ($E_i = E_f$) T -matrix in equation (10), order by order in the power counting, assuming that

$$v = v^{(0)} + v^{(1)} + v^{(2)} + \dots , \quad (12)$$

admits the same expansion with $v^{(n)}$ of order Q^n . This procedure implies that

$$v^{(0)} = T^{(0)} , \quad (13)$$

$$v^{(1)} = T^{(1)} - [v^{(0)} G_0 v^{(0)}] , \quad (14)$$

$$v^{(2)} = T^{(2)} - [v^{(0)} G_0 v^{(0)} G_0 v^{(0)}] - [v^{(1)} G_0 v^{(0)} + v^{(0)} G_0 v^{(1)}] , \quad (15)$$

$$v^{(3)} = T^{(3)} - [v^{(0)} G_0 v^{(0)} G_0 v^{(0)} G_0 v^{(0)}] - [v^{(1)} G_0 v^{(0)} G_0 v^{(0)} + \text{permutations}] - [v^{(2)} G_0 v^{(0)} + v^{(0)} G_0 v^{(2)}] - [v^{(1)} G_0 v^{(1)}] . \quad (16)$$

Since the potential is thus defined from on-shell amplitudes order by order, different off-shell extensions of the potential at a given order lead to different (on-shell) potentials at higher orders. In fact, there is an infinite class of $v^{(2)}(\nu)$ non-static corrections—labeled by the parameter ν [15, 16, 17, 6]—which, while equivalent on the energy-shell, are different off the energy-shell, and therefore lead to different potentials $v^{(3)}(\nu)$ in equation (16). However, this ambiguity is of no consequence, since it can be shown that different off-the-energy-shell extrapolations $v^{(2)}(\nu)$ and $v^{(3)}(\nu)$ are unitarily equivalent [15, 6].

The inclusion (in first order) of electromagnetic interactions in the perturbative expansion of equation (7) is straightforward: the transition operator can be expanded as

$$T_\gamma = T_\gamma^{(-3)} + T_\gamma^{(-2)} + T_\gamma^{(-1)} + \dots , \quad (17)$$

where $T_\gamma^{(n)}$ is of order eQ^n (e is the electric charge). The nuclear charge, ρ , and current, \mathbf{j} , operators follow from $v_\gamma = A^0 \rho - \mathbf{A} \cdot \mathbf{j}$, where $A^\mu = (A^0, \mathbf{A})$ is the electromagnetic vector field, and it is assumed that v_γ has a similar expansion as T_γ . The requirement that, in the context of the LS equation, v_γ matches T_γ order by order in the power counting implies the following relations:

$$v_\gamma^{(-3)} = T_\gamma^{(-3)} \quad (18)$$

$$v_\gamma^{(-2)} = T_\gamma^{(-2)} - [v_\gamma^{(-3)} G_0 v^{(0)} + v^{(0)} G_0 v_\gamma^{(-3)}] , \quad (19)$$

$$v_\gamma^{(-1)} = T_\gamma^{(-1)} - [v_\gamma^{(-3)} G_0 v^{(0)} G_0 v^{(0)} + \text{permutations}] - [v_\gamma^{(-2)} G_0 v^{(0)} + v^{(0)} G_0 v_\gamma^{(-2)}] , \quad (20)$$

$$v_\gamma^{(0)} = T_\gamma^{(0)} - [v_\gamma^{(-3)} G_0 v^{(0)} G_0 v^{(0)} G_0 v^{(0)} + \text{permutations}] - [v_\gamma^{(-2)} G_0 v^{(0)} G_0 v^{(0)} + \text{permutations}] - [v_\gamma^{(-1)} G_0 v^{(0)} + v^{(0)} G_0 v_\gamma^{(-1)}] - [v_\gamma^{(-3)} G_0 v^{(2)} + v^{(2)} G_0 v_\gamma^{(-3)}] , \quad (21)$$

$$v_\gamma^{(1)} = T_\gamma^{(1)} - [v_\gamma^{(-3)} G_0 v^{(0)} G_0 v^{(0)} G_0 v^{(0)} G_0 v^{(0)} + \text{permutations}]$$

$$\begin{aligned}
 & - \left[v_\gamma^{(-2)} G_0 v^{(0)} G_0 v^{(0)} G_0 v^{(0)} + \text{permutations} \right] \\
 & - \left[v_\gamma^{(-1)} G_0 v^{(0)} G_0 v^{(0)} + \text{permutations} \right] - \left[v_\gamma^{(0)} G_0 v^{(0)} + v^{(0)} G_0 v_\gamma^{(0)} \right] \\
 & - \left[v_\gamma^{(-3)} G_0 v^{(2)} G_0 v^{(0)} + \text{permutations} \right] - \left[v_\gamma^{(-3)} G_0 v^{(3)} + v^{(3)} G_0 v_\gamma^{(-3)} \right] , \quad (22)
 \end{aligned}$$

where $v_\gamma^{(n)} = A^0 \rho^{(n)} - \mathbf{A} \cdot \mathbf{j}^{(n)}$, $v^{(n)}$ are the NN potentials constructed in equations (13)–(16) (the ν dependence of $v^{(2)}$ and $v^{(3)}$ is understood), and use has been made of the fact that $v^{(1)}$ vanishes. In the propagator G_0 , the initial energy E_i includes the photon energy ω_γ (itself of order Q^2), since $E_i = E_1 + E_2 + \omega_\gamma = E'_1 + E'_2$, and the intermediate energy E_I may include, in addition to the kinetic energies of the intermediate nucleons, also the photon energy, depending on the specific time ordering being considered.

3. Electromagnetic current and charge operators up to one loop

The contributions to the electromagnetic current operator up to one loop, as resulting from the interaction Hamiltonians and the perturbative expansion outlined above, are illustrated diagrammatically in figure 1. Since there is no $n = -3$ contribution to \mathbf{j} the current operator is unaffected by the non-static corrections entering the potentials $v^{(2)}$ and $v^{(3)}$. The lowest order ($n = -2$) consists of the single-nucleon convection and spin-magnetization currents:

$$\mathbf{j}^{(-2)} = \frac{e}{2m} (2e_{N,1} \mathbf{K}_1 + i\mu_{N,1} \boldsymbol{\sigma}_1 \times \mathbf{q} + 1 \rightleftharpoons 2) , \quad (23)$$

where \mathbf{q} is the momentum carried by the external field, \mathbf{k}_i and \mathbf{K}_i denote the combinations of initial and final nucleon momenta $\mathbf{k}_i = \mathbf{p}'_i - \mathbf{p}_i$, $\mathbf{K}_i = (\mathbf{p}'_i + \mathbf{p}_i)/2$, and $e_{N,i}$ and $\mu_{N,i}$ have been defined in equation (5). The counting eQ^{-2} follows from the product of a factor eQ^1 associated with the γNN vertex, and a factor Q^{-3} due to the momentum-conserving δ -function implicit in a disconnected term of this type. In this one-body contribution we also include a q^2 -dependence (which would only arise at successive chiral orders) in the form of the electric and magnetic form factors, as resulting from fits of electron scattering on the proton and deuteron. We refer

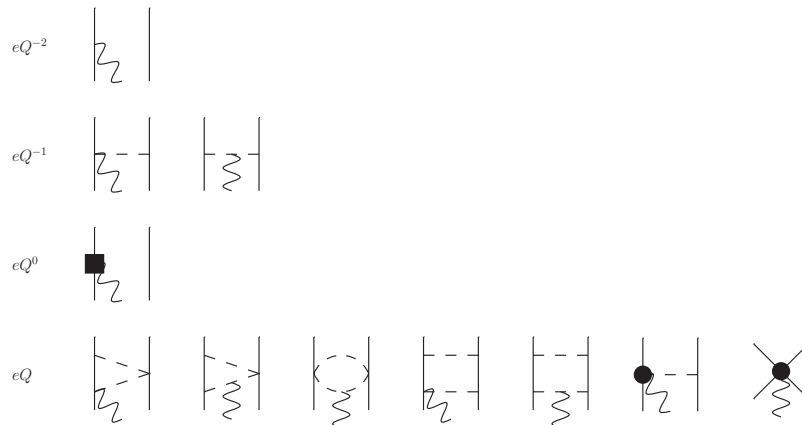


Figure 1. Diagrams illustrating one- and two-body currents entering at LO (eQ^{-2}), NLO (eQ^{-1}), N2LO (eQ^0), and N3LO (eQ^1). Nucleons, pions, and photons are denoted by solid, dashed, and wavy lines. Only the relevant topologies are indicated. Loop corrections to short-range currents turn out to vanish.

to Refs. [4, 5, 7] for the explicit expressions up to N3LO, as obtained within the formalism

outlined in section 2. They depend on the known parameters g_A and F_π (NLO and N3LO), and the nucleon's magnetic moments (LO and N2LO). Loop corrections to the short-range currents turn out to cancel [7]. Unknown LECs enter the N3LO one-pion exchange (OPE) contribution involving the $\gamma\pi N$ vertex of order $e Q^2$ from $H_{\gamma\pi N}$,

$$\mathbf{j}_{\gamma\pi N}^{(1)} = i e \frac{g_A}{F_\pi^2} \frac{\boldsymbol{\sigma}_2 \cdot \mathbf{k}_2}{\omega_{k_2}^2} \left[\left(d'_8 \tau_{2,z} + d'_9 \boldsymbol{\tau}_1 \cdot \boldsymbol{\tau}_2 \right) \mathbf{k}_2 - d'_{21} (\boldsymbol{\tau}_1 \times \boldsymbol{\tau}_2)_z \boldsymbol{\sigma}_1 \times \mathbf{k}_2 \right] \times \mathbf{q} + 1 \rightleftharpoons 2 . \quad (24)$$

The contributing LECs could be fixed by relating them, in a resonance saturation picture, to the couplings in the N to Δ excitation and $\rho\pi\gamma$ transition currents, or they could be fixed by pion photo-production data on a single nucleon or photo-nuclear data at low energies. Further LECs enter the two-contact currents, from minimal and non-minimal substitution,

$$\begin{aligned} \mathbf{j}_{\text{CT,m}}^{(1)} &= \frac{i}{16} (\boldsymbol{\tau}_1 \times \boldsymbol{\tau}_2)_z \left[[C_2 + 3C_4 + C_7 + (C_2 - C_4 - C_7) \boldsymbol{\sigma}_1 \cdot \boldsymbol{\sigma}_2] (\mathbf{k}_1 - \mathbf{k}_2) \right. \\ &\quad \left. + C_7 [\boldsymbol{\sigma}_1 \cdot (\mathbf{k}_1 - \mathbf{k}_2) \boldsymbol{\sigma}_2 + \boldsymbol{\sigma}_2 \cdot (\mathbf{k}_1 - \mathbf{k}_2) \boldsymbol{\sigma}_1] \right] \\ &\quad - \frac{i C_5}{4} (\boldsymbol{\sigma}_1 + \boldsymbol{\sigma}_2) \times (e_1 \mathbf{k}_1 + e_2 \mathbf{k}_2) , \end{aligned} \quad (25)$$

where the C_i can be taken from the NN potential, and

$$\mathbf{j}_{\text{CT,nm}}^{(1)} = -i e \left[C'_{15} \boldsymbol{\sigma}_1 + C'_{16} (\tau_{1,z} - \tau_{2,z}) \boldsymbol{\sigma}_1 \right] \times \mathbf{q} + 1 \rightleftharpoons 2 . \quad (26)$$

No three-body currents arise up to N³LO included here, due to cancellations between irreducible and recoil-corrected reducible diagrams, similarly to what happens for the three-nucleon force.

Diagrams contributing to the charge operators $\rho^{(n)}$ up to order $e Q^1$ (N4LO) included are illustrated in figure 2. The leading contribution, of order $e Q^{-3}$, is a one-body operator and results from the first term of the γN interaction Hamiltonian in equation (2),

$$\rho^{(-3)} = e e_{N,1} + 1 \rightleftharpoons 2 , \quad (27)$$

and, as before, electric form factors can be included, even if they would arise at successive chiral orders. There are no NLO ($e Q^{-2}$) contributions, whereas at N2LO there is a relativistic correction of order $(Q/m)^2$ to the LO charge operator, which results from the second line of equation (2). At this order, there are in principle also a pion-in-flight term, which, however, turns out to vanish when the contributions of the six time-ordered diagrams, evaluated in the static limit, are summed up, and a OPE contribution, which vanishes due to a similar cancellation. The power counting is different from the current operator, for which the LO term is of order $e Q^{-2}$ (in the two-nucleon system), i.e. it is suppressed by an extra power of Q relative to $\rho^{(-3)}$, and where there are NLO ($e Q^{-1}$) corrections involving seagull and in-flight contributions associated with OPE, which have no counterpart in the present case. The pion-in-flight and OPE diagrams also lead to N3LO contributions due to non-static corrections resulting from the expansion of the denominators involving pion energies as in equation (9). In particular, the specific form of the N3LO charge operator depends on the (non-unique) off-the-energy shell prescription adopted for the non-static piece in the OPE potential [6]. The same applies to part of the N4LO contributions. This ambiguity in the non-static OPE and two-pion exchange (TPE) potentials and accompanying charge operators is of no consequence, however, since different form for these are related to each other by a unitary transformation [6, 7]. Thus, provided a consistent set is adopted, predictions for physical observables, such as the few-nucleon charge form factors, will

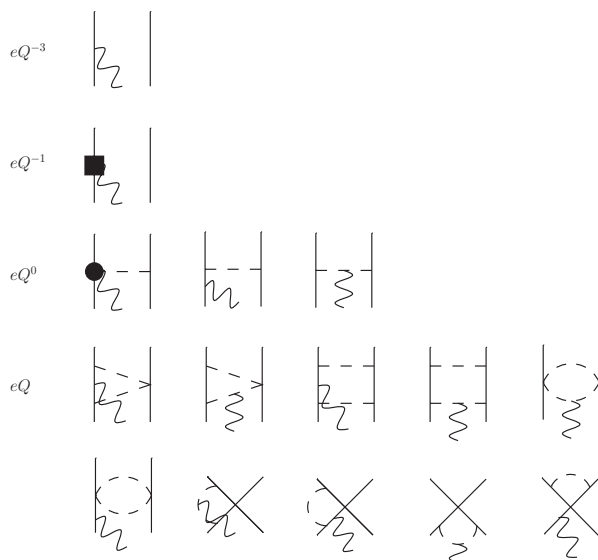


Figure 2. Diagrams illustrating one- and two-body charge operators entering at LO (eQ^{-3}), N2LO (eQ^{-1}), N3LO (eQ^0), and N4LO (eQ^1). The square represents the $(Q/m)^2$, or $(v/c)^2$, relativistic correction to the LO one-body charge operator, whereas the solid circle is associated with a $\gamma\pi N$ charge coupling of order eQ . Only the relevant topologies are indicated.

remain unaffected by the non-uniqueness associated with off-the-energy-shell effects. Finally, charge conservation,

$$\rho(\mathbf{q} = 0) = \int d\mathbf{x} \rho(\mathbf{x}) = e (e_1 + e_2) , \quad (28)$$

where $\rho(\mathbf{x})$ and $\rho(\mathbf{q})$ denote, respectively, the charge density and its Fourier transform, implies that the charge operators $\rho^{(n \geq -2)}(\mathbf{q})$ vanish at $\mathbf{q} = 0$. This latter requirement is satisfied by the operators illustrated in figure 2, regardless of the adopted off-the-energy shell prescription [6]. We also emphasize that, up to N4LO included, there are no unknown LECs. As a consequence, the loop integrals entering diagrams at N4LO, although individually ultra-violet divergent, sum up to give a finite result.

4. Fixing the LECs

The operators described in the previous section depend on the LECs C_i entering the two-nucleon contact Lagrangian through the minimal coupling procedure, on the non-minimal coupling LECs C'_{15} and C'_{16} and on the subleading pion-nucleon couplings d'_i entering in the one-pion exchange N3LO current. The latter could be fitted to pion photo-production data on a single nucleon, which however involve photon energies much higher than those relevant for the threshold processes under consideration here, or related to hadronic coupling constants through resonance saturation. We prefer to treat them as fitting parameters. In Refs. [18, 7] we explored different strategies to such fitting procedure. It turns out that the most effective one is to use Δ -resonance saturation for the isovector pion-nucleon couplings in equation (24),

$$d'_8 = 4d'_{21} = \frac{4\mu_{\gamma N\Delta} h_A}{9m_N(m_\Delta - m_N)} \quad (29)$$

where $\mu_{\gamma N\Delta} \sim 3\mu_N$ is the $N\Delta$ transition magnetic moment and h_A the $\pi N\Delta$ coupling constant, $h_A/f_\pi = f_{\pi N\Delta}/m_\pi$ with $f_{\pi N\Delta}^2/(4\pi) = 0.35$. We are then left with 3 parameter, one isovector

and two isoscalar,

$$C'_{15} = d_1^S/\Lambda^4, \quad d'_9 = d_2^S/\Lambda^2, \quad C'_{16} = d_1^V/\Lambda^4, \quad (30)$$

The isoscalar LECs can be fixed from the magnetic moments of the deuteron and the isoscalar combination of the trinucleon. The isovector LEC can be fixed from the isovector trinucleon magnetic moment or from the np thermal radiative capture cross section. Nuclear wave functions are taken from the Hyperspherical Harmonic method [19], using either the Argonne v_{18} (AV18) [20] or the Idaho chiral N3LO [21] two-nucleon potentials for $\Lambda = 500, 600$ MeV [22]. For $A = 3$ we also included, respectively, the Urbana IX [23] and chiral N2LO [24, 25] with the intervening LECs c_D and c_E fixed from the trinucleon binding energies and the ${}^3\text{H}$ Gamow-Teller matrix element [26]. Electromagnetic matrix elements are calculated with MonteCarlo methods, with statistical uncertainties of less than 1%.

The cumulative contributions to the observables used to fix the LECs are shown in figures 3 and 4. It can be seen that the convergence pattern of the chiral series is reasonable. In the

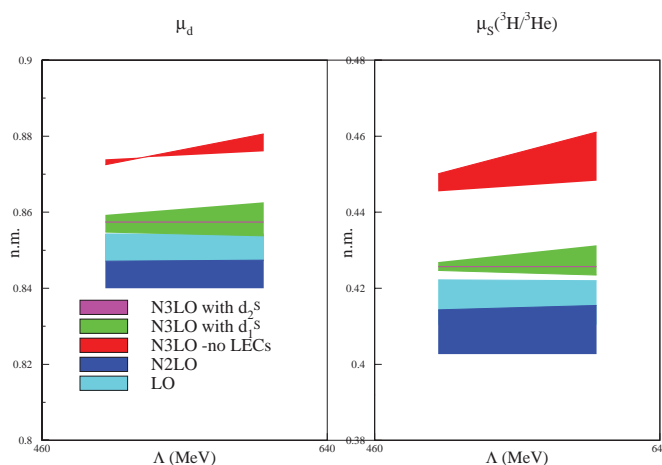


Figure 3. (Color online) Cumulative contributions to the deuteron and trinucleon (isoscalar) magnetic moments. The bands represent the variation with the two nuclear Hamiltonian model.

isovector case, depending on the strategy, either one of the two observables is in fact a prediction, which then turns out to be accurate to 2% for μ_V and 1% for σ_{np} , with a marginal dependence on the cutoff and on the Hamiltonian model. We will describe results with the latter strategy (using μ_V to constrain the LEC), which also proved effective in a recent investigation of magnetic moments and transitions in nuclei with $A \leq 9$ [27], using quantum Montecarlo techniques.

5. Results

In figure 5 we show the charge monopole and quadrupole form factors of the deuteron, confronted to the results extracted from unpolarized and tensor-polarized deuteron data.

For each interaction model also the leading order results in the expansion of the charge operator are shown. The chiral expansion stops at N3LO in this case, since the loop contribution is of isovector character. We observe very good agreement with data up to quite large momentum transfers. The cutoff dependence is larger for the chiral potentials, and does not decrease as we increase the order in the chiral expansion of the charge operator. This is a general feature that we observe. We therefore conclude that the Λ -dependence is mainly due to the interaction potentials, and that the scheme differences in the derivation of the potentials and the transition operator are important. This means that also the calculations with the chiral potentials should

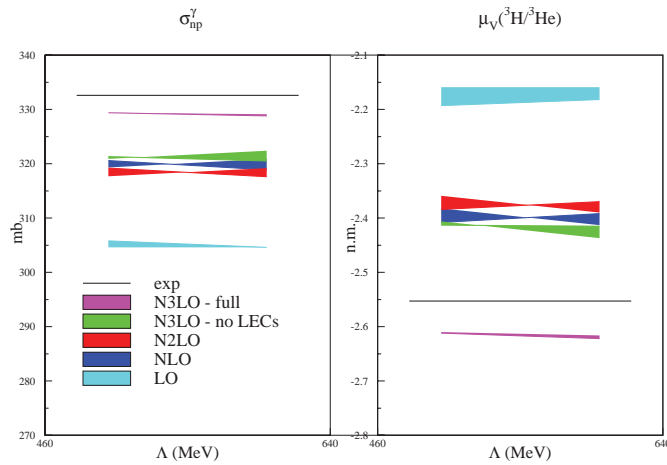


Figure 4. (Color online) Cumulative contributions to the isovector trinucleon magnetic moment and to the np radiative capture cross sections. The black line indicates the experimental value. Notations as in figure 3.

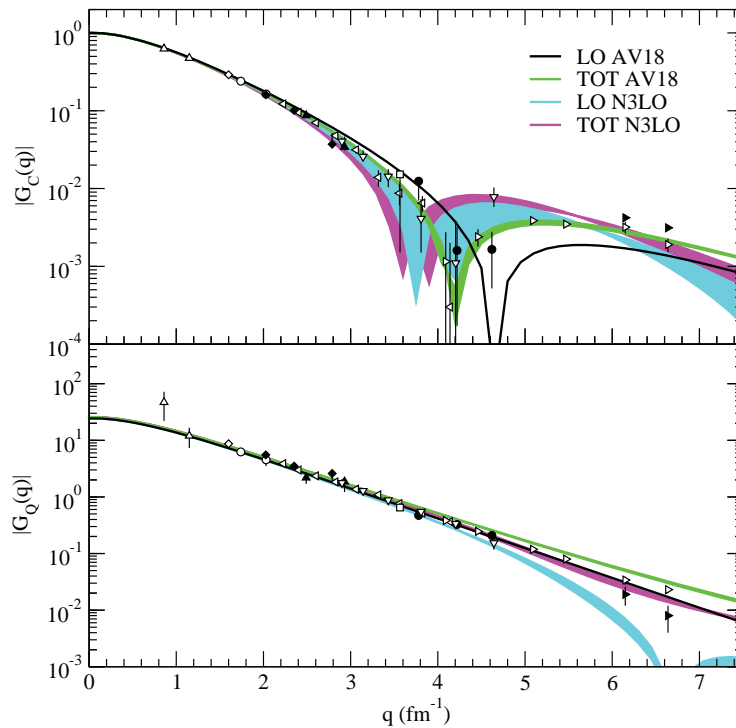


Figure 5. (Color online) Deuteron charge and quadrupole form factors at leading order (LO) and including all subleading terms up to N3LO (TOT), for the two interaction models. The bands represent the variation with the cutoff Λ between 500 and 600 MeV. The experimental data are from Refs. [28, 29, 30, 31, 32, 33, 34, 35, 36, 37, 38, 39, 40, 41, 42, 43, 44, 45, 46, 47, 48, 49].

be considered as being of hybrid character. On the contrary, we checked that the impact of the

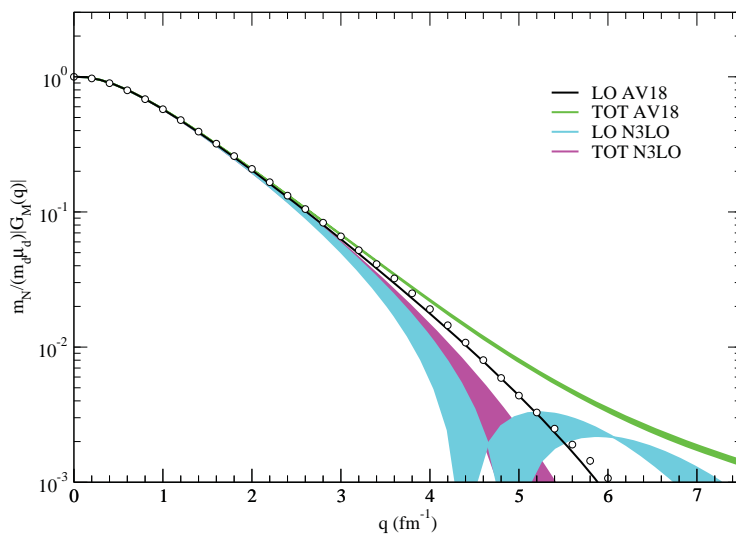


Figure 6. (Color online) Deuteron magnetic form factor, notations as if figure 5. Experimental data are from Refs. [28, 34, 50, 35, 51, 52].

off-shell ambiguity, discussed earlier is negligible.

The magnetic form factor is plotted in figure 6. The correct normalization is imposed in this case by our procedure for fixing the isoscalar LECs. The agreement between theory and experiment extends to momenta of order 2-3 fm^{-1} , depending on the interaction model. In figure 7 we show the charge form factors for ${}^3\text{He}$ and ${}^3\text{H}$. In this case also the chiral loops contribute at N4LO. The interaction potentials also include the corresponding three-nucleon forces. We observe a large effect of two-body contributions, which bring theory closer to experiment in the diffraction region. By examining separately the individual contributions in the chiral series, however, there is no clear sign of convergence for momenta larger than 3 fm^{-1} , as the contributions at N3LO and N4LO are of comparable size, and much larger than the N2LO. Finally, in figure 8, we show the magnetic form factors of trinucleons, whose isoscalar combination is used to fix one the relevant LECs. The agreement with data is very good up to momenta $\sim 2 \text{ fm}^{-1}$. Also in this case the role of the two-body contributions is crucial in bringing theory closer to data, but the diffraction region is still problematic.

6. Conclusions

Chiral perturbation theory, in conjunction with accurate ab-initio techniques to describe light nuclei, allows to make sharp predictions for nuclear electromagnetic observables in the low-energy domain. We have described our formalism to derive the nuclear current and charge operators up to one loop order of the chiral expansion, based on the requirement that, when iterated in the Lippman-Schwinger equation, they lead to the same transition amplitude obtained within time-ordered perturbation theory, order by order in the chiral expansion.

The issue of the convergence pattern of the chiral expansion and of the naturalness of the relevant LECs, however, deserves further investigation, in particular for what concerns the role of the Δ resonance and its possible inclusion within the effective theory.

References

- [1] Gasser J and Leutwyler H 1984 *Annals Phys.* **158** 142
- [2] Weinberg S 1990 *Phys. Lett. B* **251** 288; 1991 *Nucl. Phys. B* **363** 3; 1992 *Phys. Lett. B* **295** 114

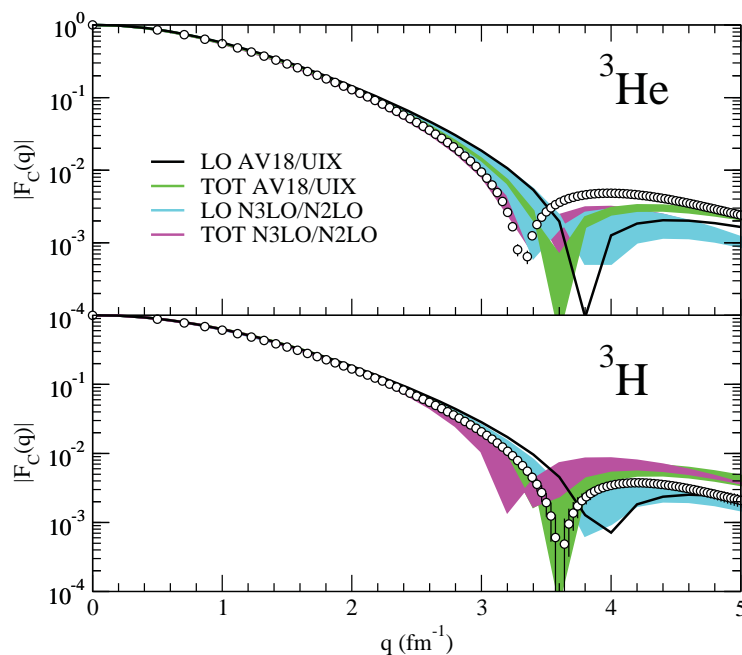


Figure 7. (Color online) Charge form factors of ${}^3\text{He}$ and ${}^3\text{H}$. Notations as in figure 5. Experimental data are from Refs. [53].

- [3] Park T -S, Min D -P, and Rho M 1996 *Nucl. Phys. A* **596** 515
- [4] Pastore S, Schiavilla R, and Goity J L 2008 *Phys. Rev. C* **78** 064002
- [5] Pastore S, Girlanda L, Schiavilla R, Viviani M, and Wiringa R B 2009 *Phys. Rev. C* **80** 034004
- [6] Pastore S, Girlanda L, Schiavilla R, and Viviani M 2011 *Phys. Rev. C* **84** 024001
- [7] Piarulli M, Girlanda L, Marcucci L E, Pastore S, Schiavilla R, and Viviani M 2013 *Phys. Rev. C* **87** 014006
- [8] Kölling S, Epelbaum E , Krebs H, and Meissner U -G 2009 *Phys. Rev. C* **80** 045502
- [9] Kölling S, Epelbaum E, Krebs H, and Meissner U -G 2011 *Phys. Rev. C* **84** 054008
- [10] Epelbaum E, Glöckle W, and Meissner U -G 1998 *Nucl. Phys. A* **637** 107; 2000 *Nucl. Phys. A* **671** 295; 2003 *Nucl. Phys. A* **714** 535; 2005 *Nucl. Phys. A* **747** 362
- [11] Okubo S 1954 *Prog. Theor. Phys.* **12** 603
- [12] Bernard V 2008 *Prog. Part. Nucl. Phys.* **60** 82
- [13] Girlanda L, Pastore S, Schiavilla R, and Viviani M 2010 *Phys. Rev. C* **81** 034005
- [14] Gezerlis A, Tews I, Epelbaum E, Gandolfi S, Hebeler K, Nogga A, and Schwenk A 2013 *Phys. Rev. Lett.* **111** 032501
- [15] Friar J L 1977 *Annals Phys.* **104** 380
- [16] Friar J L 1980 *Phys. Rev. C* **22** 796
- [17] Adam J, Goller H, and Arenhövel H 1993 *Phys. Rev. C* **48** 370
- [18] Girlanda L, Kievsky A, Marcucci L E, Pastore S, Schiavilla R, and Viviani M 2010 *Phys. Rev. Lett.* **105** 232502
- [19] Kievsky A *et al.* 2008 *J. Phys. G* **35** 063101
- [20] Wiringa R B, Stoks V G J, and Schiavilla R 1995 *Phys. Rev. C* **51** 38
- [21] Entem D R and Machleidt R (2003) *Phys. Rev. C* **68** 041001
- [22] Machleidt R and Entem D R 2011 *Phys. Rep.* **503** 1
- [23] Pudliner B S *et al.* 1997 *Phys. Rev. C* **56** 1720
- [24] Epelbaum E, Nogga A, Gloeckle W, Kamada H, Meissner U -G, and Witala H 2002 *Phys. Rev. C* **66** 064001
- [25] Navratil P 2007 *Few-Body Syst.* **41** 117
- [26] Marcucci L E, Kievsky A, Rosati S, Schiavilla R, and Viviani M 2012 *Phys. Rev. Lett.* **108** 052502
- [27] Pastore S, Pieper S C, Schiavilla R, and Wiringa R B 2013 *Phys. Rev. C* **87** 035503
- [28] Buchanan C D and Yearian M R 1965 *Phys. Rev. Lett.* **15** 303
- [29] Benaksas D, Drickey D, and Frèrejacque D 1966 *Phys. Rev.* **148** 1327
- [30] Elias J E *et al.* 1969 *Phys. Rev.* **177** 2075

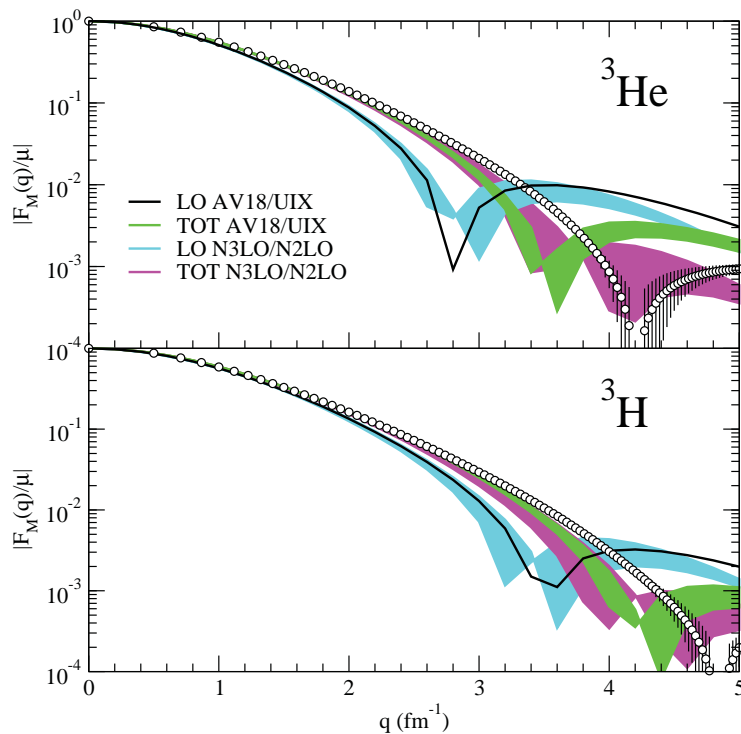


Figure 8. (Color online) Magnetic form factors of ${}^3\text{He}$ and ${}^3\text{H}$. Notations as in figure 5. Experimental data are from Refs. [53].

- [31] Galster S *et al.* 1971 *Nucl. Phys. B* **32** 221
- [32] Berard R W *et al.* 1973 *Phys. Lett. B* **47** 355
- [33] Arnold R G *et al.* 1975 *Phys. Rev. Lett.* **35** 776
- [34] Simon G G , Schmitt C, and Walther V H 1981 *Nucl. Phys. A* **364** 285
- [35] Cramer R *et al.* 1985 *Z. Phys. C* **29** 513
- [36] Platchkov S *et al.* 1990 *Nucl. Phys. A* **510** 740
- [37] Abbott D *et al.* 1999 *Phys. Rev. Lett.* **82** 1379
- [38] Alexa L C *et al.* 1999 *Phys. Rev. Lett.* **82** 1374
- [39] Schulze M E *et al.* 1984 *Phys. Rev. Lett.* **52** 597
- [40] The I *et al.* 1991 *Phys. Rev. Lett.* **67** 173
- [41] Zhang C *et al.* 2011 *Phys. Rev. Lett.* **107** 252501
- [42] Dmitriev V F *et al.* 1985 *Phys. Lett. B* **157** 143
- [43] Wojtsekhowski B B *et al.* 1986 *Pis'ma Zh. Eksp. Teor. Fiz.* **43** 567
- [44] Gilman R *et al.* 1990 *Phys. Rev. Lett.* **65** 1733
- [45] Nikolenko D M *et al.* 2003 *Phys. Rev. Lett.* **90** 072501
- [46] Boden B *et al.* 1991 *Z. Phys. C* **49** 175
- [47] Ferro-Luzzi M *et al.* 1996 *Phys. Rev. Lett.* **77** 2630
- [48] Bouwhuis M *et al.* 1999 *Phys. Rev. Lett.* **82** 3755
- [49] Abbott D *et al.* 2000 *Phys. Rev. Lett.* **84** 5053
- [50] Auffret S *et al.* 1985 *Phys. Rev. Lett.* **54** 649
- [51] Bosted P E *et al.* 1990 *Phys. Rev. C* **42** 38
- [52] Sick I 2001 *Prog. Part. Nucl. Phys.* **47** 245
- [53] Amroun A *et al.* 1994 *Nucl. Phys. A* **579** 596